

**He Bulge Revealed: He and CO<sub>2</sub> diurnal and seasonal variations in the Upper Atmosphere of Mars as detected by MAVEN NGIMS**

Elrod, M.K.<sup>1,2</sup>, Bougher, S.<sup>3</sup>, Bell, J.<sup>4</sup>, Mahaffy, P. R.<sup>1</sup>, Benna, M.<sup>1,5</sup>, Stone, S.<sup>6</sup>, Yelle, R.<sup>6</sup>, Jakosky, B.<sup>7</sup>.

<sup>1</sup> NASA Goddard Space Flight Center, Greenbelt, MD 20771

<sup>2</sup> CRESST, University of Maryland, College Park, MD

<sup>3</sup> Climate and Space Sciences and Engineering Department, University of Michigan, Ann Arbor, MI

<sup>4</sup> National Institute of Aerospace, Hampton, VA

<sup>5</sup> CRESST, University of Maryland Baltimore County, Baltimore, MD

<sup>6</sup> Lunar and Planetary Laboratory and Department of Planetary Sciences, University of Arizona, Tucson, AZ, USA

<sup>7</sup> Laboratory for Atmospheric and Space Physics, University of Colorado, Boulder, CO

**Key Points**

1. Data using MAVEN NGIMS for nearly one Martian year reveal Diurnal and seasonal variations in He and CO<sub>2</sub> indicating a changing He bulge in Martian upper atmosphere.

This is the author manuscript accepted for publication and has undergone full peer review but has not been through the copyediting, typesetting, pagination and proofreading process, which may lead to differences between this version and the [Version of Record](#). Please cite this article as doi: [10.1002/2016JA023482](https://doi.org/10.1002/2016JA023482)

2. Observed He bulge is found to agree preliminarily with M-GITM modeling efforts.
3. He bulge found at Mars is similar to those found at Earth and Venus

### **Abstract**

Analysis of the Neutral Gas and Ion Mass Spectrometer (NGIMS) on the Mars Atmosphere Volatiles and Evolution (MAVEN) spacecraft closed source data from all orbits with good pointing revealed an enhanced Helium [He] density on the night-side orbits and a depressed He density on the dayside by about a factor of 10-20. He was also found to be larger in the polar regions than in the equatorial regions. The northern polar winter nightside He bulge was approximately twice that of the northern polar summer nightside bulge. The first six weeks of the MAVEN prime mission had periapsis at high latitudes on the night-side during northern winter, followed by the mid latitudes on the dayside moving to low latitudes on the night-side returning to the high latitudes during northern summer. In this study we examined the NGIMS data not only in the different latitudes but sorted by Ls in order to separate the diurnal or local solar time (LST) effects from the seasonal effects. The Mars Global Ionosphere Thermosphere Model (M-GITM), has predicted the formation of a He bulge in the upper atmosphere of Mars on the night-side early morning hours ( $L_s = 2 - 5$  h) with more He collecting around

the poles. Taking a slice at constant altitude across all orbits indicates corresponding variations in He and CO<sub>2</sub> with respect to LST and Ls and a diurnal and seasonal dependence.

Author Manuscript

## 1. Introduction

Helium [He] in the terrestrial atmospheres of Venus, Earth, and Mars can be used as a tracer for vertical advection and wind currents in the upper atmosphere. Vertical advection and neutral winds are very difficult to directly measure and have mainly been modeled.

The Mars Atmosphere and Volatiles Evolution (MAVEN) [Jakosky *et al.*, 2014] spacecraft has been in orbit around Mars since September 2014 observing the upper atmosphere. The Neutral Gas Ion Mass Spectrometer (NGIMS) [Mahaffy *et al.*, 2014] began operations in late October 2014 with observations during the encounter of Comet Siding Spring and regular science operations beginning in Nov 2014. Within the prime mission (Nov, 2014- Dec 2015) MAVEN performed four deep dips and in the extended mission (Jan 2016-Aug 2016) the spacecraft performed two more deep dips where the spacecraft passed lower into the atmosphere than its normal operations, closer to ~120 km.

During its normal operations MAVEN periapsis altitude is generally around 150 km allowing it to measure the traditional exobase region near 200 km. MAVEN began the science mission in the northern polar region remaining above 45° N from Ls 216 – 262 and 88 - 150, was in the equatorial region (between latitude 45° N and -45° S) from Ls =

289 – 339, 50-100 and 150-189, and dipped into the southern polar region (latitude < 45° S) from Ls 331-50. This has provided the opportunity to examine the northern polar region at winter and summer, the southern polar region during equinox and the equatorial region through equinox and near the two solstices. By sorting the data into northern and southern polar regions and equatorial regions, we are better able to examine diurnal and possible seasonal effects.

For this study, we are focusing mainly on the diurnal and seasonal variations of the He density measured at 4 Dalton (Da) and CO<sub>2</sub> secured by using measurements at 44 Da or at fragment or isotope masses in those cases where the 44 signal saturated the detector. The 44 Da signal can also be attenuated to enable this measurement at lower altitudes. Predictions from the three-dimensional Mars Global Ionosphere Thermosphere Model (M-GITM), [Bougher *et al.*, 2015, JGR, 120, 311] indicate that He densities should be enhanced on the night-side (LST = 2 – 5 h) and around the poles, in contrast to lower densities on the dayside or around the equator. At Ls = 90 and 270 (solstices), the He bulge is expected to be highest on the night-side southern and northern poles respectively. At Ls = 0 and 180 (equinoxes), the He bulge is expected to be highest near dawn at mid-latitudes. He peaks in the equatorial region are expected to occur near equinox as the bulge is shifting from one pole to the other [Bell *et al.*, 2015, Kasprzak *et al.*, 1993].

He bulges have been detected at Earth, Venus, and now confirmed at Mars. Earlier observations of the Venus atmosphere by the Pioneer Venus mission indicate that there is a significant day/night variation in the He densities [Neimann et al., 1980]. Observations of He, prior to MAVEN, in the Martian atmosphere were limited to the dayside and, thus, the day/night variations were theorized based on the observations made at Venus [Krasnopolsky 2002, 1986, Bougher 1986, Bougher et al, 2003]. Previous observations of He in the Martian atmosphere conducted by the Viking lander upon entry [Kasprzak et al., 1993, Nier and McElroy, 1977]. MAVEN is the first orbiter at Mars with the capabilities necessary to observe the He atmosphere down to ~120 km. At Earth, He was found to be dependent on the local vertical advection and molecular diffusion in the upper atmosphere [Liu et al., 2014, Sutton et al., 2015]. The upward summer winds depress the He density while the downward winter winds greatly increase the He density in the upper atmosphere above the homopause. This driving force causes the He to collect in the upper latitudes creating a He bulge.

### **2.1—Methods: NGIMS Data**

NGIMS is a quadrupole mass spectrometer (qms) designed to measure neutral gas from 2-150 Da. It has the ability to attenuate the sensor, twice, when the detector becomes saturated. The maximum counts per second (cps) that the detector is able to read before saturation is  $\sim 10^7$ . We have the capability of detuning the focusing lenses

such that the signal will be attenuated by a factor of  $\sim 10$  and a factor of  $\sim 100$  at each detuning. This allows the qms to detect densities to much higher concentrations particularly for Ar and CO<sub>2</sub> which will typically saturate the detector at our nominal attenuation as primary constituents of the upper atmosphere will reach densities  $\sim 10^{10}$ - $10^{11}$  part/cc for CO<sub>2</sub>. The high concentration of Ar, CO<sub>2</sub>, and the subspecies CO and O in the atmosphere, m44, m16, m28, and m40, amongst a few others, will consistently saturate the un-attenuated detector. Therefore, it is necessary to correct the saturated masses with the attenuated signals. While CO<sub>2</sub> and Ar will saturate and need to be corrected, He never saturates the detector and thus is uncorrected other than for background counts. In this paper we focus on background subtracted and corrected masses 4 and 44. In addition, NGIMS alternates between a closed source mode and an open source mode. On a normal science run, the closed source neutral mode is run every orbit, for consistency and calibration. Because we can directly calibrate the sensitivity of the closed source, we use this mode to compute the abundances for the non-reactive species Ar, He, CO<sub>2</sub>, N<sub>2</sub>, and CO. The open source mode will alternate between neutral beaming mode and filaments off for ion mode. For this study, since we are using only He and CO<sub>2</sub>, we are able to use the closed source data, which are run every orbit.

We used data from October 18, 2014, obtained during the encounter with Comet Siding Spring, through August 4, 2016, MAVEN NGIMS level 2 version 06 revision 02 neutral data. In order to reduce instrumentation effects all data are restricted to the inbound portion of the pass. While He is non-reactive to the interior of the instrument CO<sub>2</sub> reacts with the interior of the instrument and has a much higher background on the outbound. This made for inconsistent He/CO<sub>2</sub> ratios between inbound vs. outbound due to an instrumental effect rather than an atmospheric effect. Note: All NGIMS data are in IAU coordinates and altitude is measured to the Martian Aeroid not the surface.

We binned the data in the following manner: altitude (alt) in 1 km steps from 150 km to 350 km, local solar time (LST) in 1 hour steps from 0 h to 24 h, and latitude in 6° steps from -90° to 90°. In addition, we took a slice of the data at a constant altitude of 200 km in order to compare the variations in the He density over time, latitude and LST by removing altitude variations. We chose to use LST for our analysis because it is easier to demonstrate dawn vs. dusk asymmetry in the CO<sub>2</sub> and He densities. The M-GITM model predicts the He bulge will collect at the poles and around LST = 2 – 5 h. Figure 1 depicts the He density over all altitudes vs LST (a) and slices around the northern pole LAT > 45° N (b) southern pole LAT < -45° (c) and equatorial region between LAT 45° and -45° (d). In each of these panels the peak He density occurs in the region of LST = 2 – 5 h with a secondary peak around LST = 22 – 24 h.



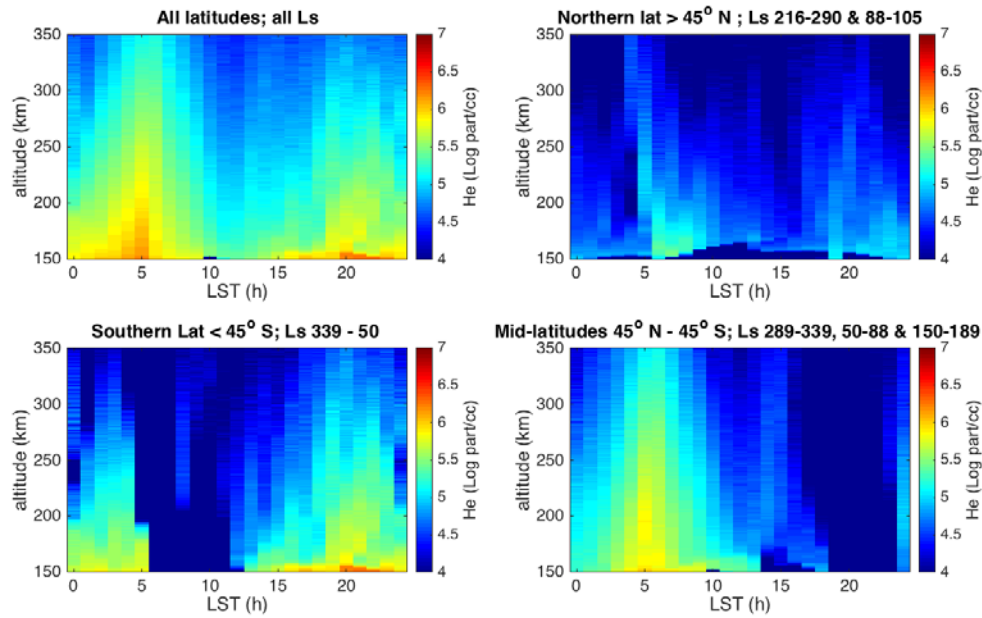


Figure 1—LST v. ALT (a) LST vs Altitude (alt) for all orbits from 150 km to 350 km in 1 km steps from 0 to 24 hour in 1 hr steps. (b) Selecting data with latitudes above  $45^{\circ}$  focusing on the He collecting around the northern polar region. (c) Selecting data with latitudes below  $-45^{\circ}$  focusing on the southern polar region. (d) All remaining data between latitudes  $45^{\circ}$  and  $-45^{\circ}$  creating an equatorial band, less likely to be affected by seasonal effects, but still highly affected by LST. All four panels indicate a peak around 2 – 5 h LST and a secondary peak around 20-21 h. The peak at 5 h is approximately 20 times higher than the data at 12 h while the peak at 20 h is approximately 10 times higher.

In figure 2 we took a single inbound vertical profile slice from two different orbits in order to compare the  $\text{CO}_2$  and He from dayside to nightside. Dayside orbit 931 ( $\text{CO}_2$  red  $\ominus$ , He green  $\circ$ ) shows a higher  $\text{CO}_2$  scale height, and higher  $\text{CO}_2$  abundance above 150 km. Conversely the He abundance is barely above noise level and it is difficult to

determine a scale height. Nightside orbit 3209 (CO<sub>2</sub> blue ✕, He purple x) shows just the opposite. CO<sub>2</sub> has a much lower scale height with abundances lower below 150km, while He abundances are much higher, well above any possible background noise levels. The He scale height is still difficult to determine, but the profile is less noisy than the dayside counterpart. With CO<sub>2</sub> being the most abundant species in the atmosphere we compared He/CO<sub>2</sub> in order to be able to track the He bulge over seasonal expansion/contraction of the atmosphere. Figure 4 tracks the ratio of He/CO<sub>2</sub> with LST and demonstrates how the diurnal effects on the bulge enhance the He densities particularly at the poles.

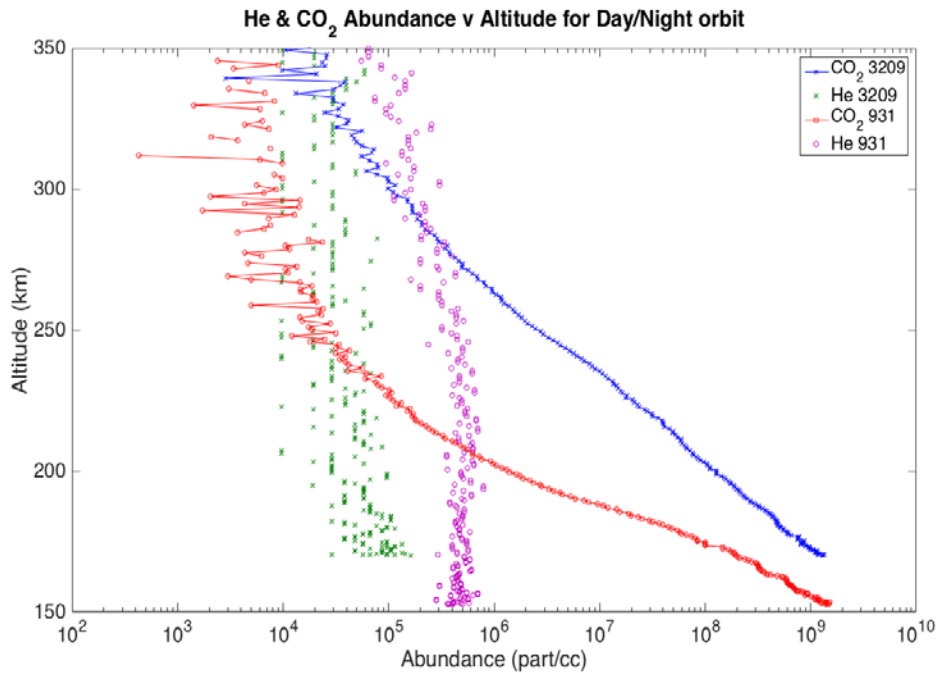


Figure 2—One nightside (931) and one dayside (3209) altitude vs abundance profile from 150 to 350 km for CO<sub>2</sub> and He on the inbound portion of the orbit. X markers are for dayside orbit 3209 LST = 13 – 14 h blue connected for CO<sub>2</sub> and green no line for He. Open circles are for nightside orbit 931 LST = 4 – 6 h, red connected for CO<sub>2</sub> and magenta no line for He.

MAVEN has been in orbit around Mars for nearly one Martian year starting at Ls = 216 to Ls = 198. MAVEN started the mission in the northern polar region from Ls = 216 – 262, during northern winter. The second pass in the northern polar region was from Ls = 88 – 150, during northern summer (Figure 1c). While the first pass was during commissioning, and there were several data gaps due to spacecraft safing events early in the mission, the second pass was complete and thus, coverage of the north polar region is adequate to determine a He Bulge on the night side with a winter enhancement. MAVEN sampled the southern polar region around Ls = 331 – 50 during equinox. The coverage in the southern polar region did show a peak during the night side, however, there was inadequate coverage on the dayside during this portion of the campaign to show a significant contrast to the nightside southern polar region, or to make any seasonal conclusions in the south. The southern polar region did show a substantial nightside enhancement compared with dayside measurements in agreement with a diurnal driver. Due to Mars' large eccentricity, it would not be surprising to see different characteristic He signatures in the northern and southern polar regions. It is possible with a longer and more pronounced southern winter, the He bulge could

accumulate more in southern winter. More data would need to be obtained to support this theory. It is our recommendation that while this data does support a strong He bulge in the southern polar region driven by diurnal effects, and the He density does appear to be higher than the northern polar region, that more data in the southern region is needed to confirm our hypothesis.

A peak in He abundances was also observed on the nightside in the equatorial region. The remainder of the data taken between  $\pm 45^\circ$  N and  $45^\circ$  S supports the strong diurnal effects with a secondary seasonal driver. This bulge was most obvious, however, closest to the southern bulge near equinox, when the bulge is likely to be shifting in intensity from one pole to the other. Figure 3 takes a slice of the He density at a constant altitude of 200 km and plots values along time (orbit #), LST, and Ls. Vertical lines are included to mark where Ls 0, 90, 180 and 270 occur along the orbit number track for reference. By taking a slice at constant altitude, it is possible to examine the variations in the atmosphere eliminating any altitude effects due to the He large scale height. Figure 4 shows the strong diurnal effect leading to the primary He density peaks at LST  $\sim 2 - 5$  hr.

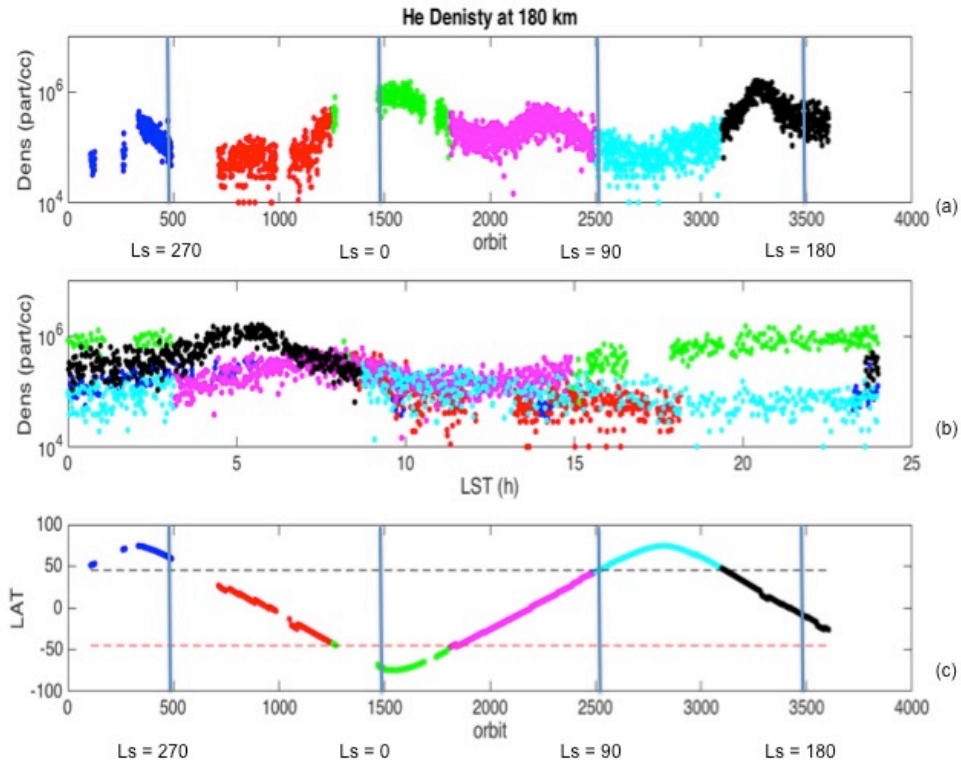


Figure 3: Vertical lines mark  $L_s = 0^\circ$ ,  $90^\circ$ ,  $180^\circ$ , and  $270^\circ$  with the colors set by latitudes measured as illustrated in (c). (a) He density at 180 km plotted over time (orbit number). Gaps in the data are due to spacecraft entering safe mode and solar conjunction. (b) He density vs LST at 200 km. Peak at LST = 2 – 5 h with a second peak around LST = 20 h. The split in the data around LST = 20 h is due to latitude differences. (c) latitude vs. orbit number to illustrate the track of the orbit and track  $L_s$ . Each region is broken up along  $45^\circ\text{N}$  and  $45^\circ\text{S}$  indicated by the black and red dashed line in (c).

In order to better understand the diurnal effects, we examined the changes in the  $\text{CO}_2$  densities as well as how they are related to the He densities with respect to LST. The  $\text{CO}_2$  atmosphere fluctuates primarily with the atmospheric neutral temperature,

i.e., as the temperatures cool (especially on the nightside), the atmospheric column contracts, and the CO<sub>2</sub> thermospheric densities decrease at a constant altitude. Conversely, as temperatures warm (generally on the dayside), the atmospheric expands and thermospheric CO<sub>2</sub> densities increase. This is opposite to the He density variation of the upper atmosphere (above the homopause). As He is a light species (with a correspondingly large scale height), its horizontal distribution may be driven by local vertical advection resulting from the thermospheric circulation pattern similar to Earth [e.g. *Lui et al.*, 2014]. Whereas, the He, due to its very high scale height and escape rate is not significantly affected by the atmospheric heating and cooling, but is more affected by the winds. He is preferentially enhanced on the nightside where it collects in those regions where the horizontal winds converge and vertical downwelling is strongest. This combination of He and CO<sub>2</sub> variations yields a useful diagnostic that clearly isolates the He bulges; i.e. the ratio of He/CO<sub>2</sub> reveals 'hot spots' indicative of these bulges. Figure 4 tracks the ratio of He/CO<sub>2</sub>, at 200 km in order to demonstrate this strong diurnal dependence with seasonal enhancement. Similarly to figure 3, each region (northern, southern and equatorial) are color coded in order to make the ratio easy to track in term of LST and past LS and orbit number. Figure 4a compares to orbit number, (b) LST, and (c) orbit vs. LAT, vertical lines mark the Ls = 0, 90, 180, and 270 in the same way as figure 3. This again reveals the same peaks seen before near LST 2 – 5. When comparing

the two northern regions (blue and cyan) this ratio has two distinct behaviors considering both can be comparable in terms of similar LST. This indicates in the northern region there was a seasonal enhancement to the bulge. The much higher peaks around  $L_s = 90$  and  $180$  are most likely due to the dominance of a diurnal effect with a slight influence from a seasonal effect. More data with better coverage will help to determine the effect better.

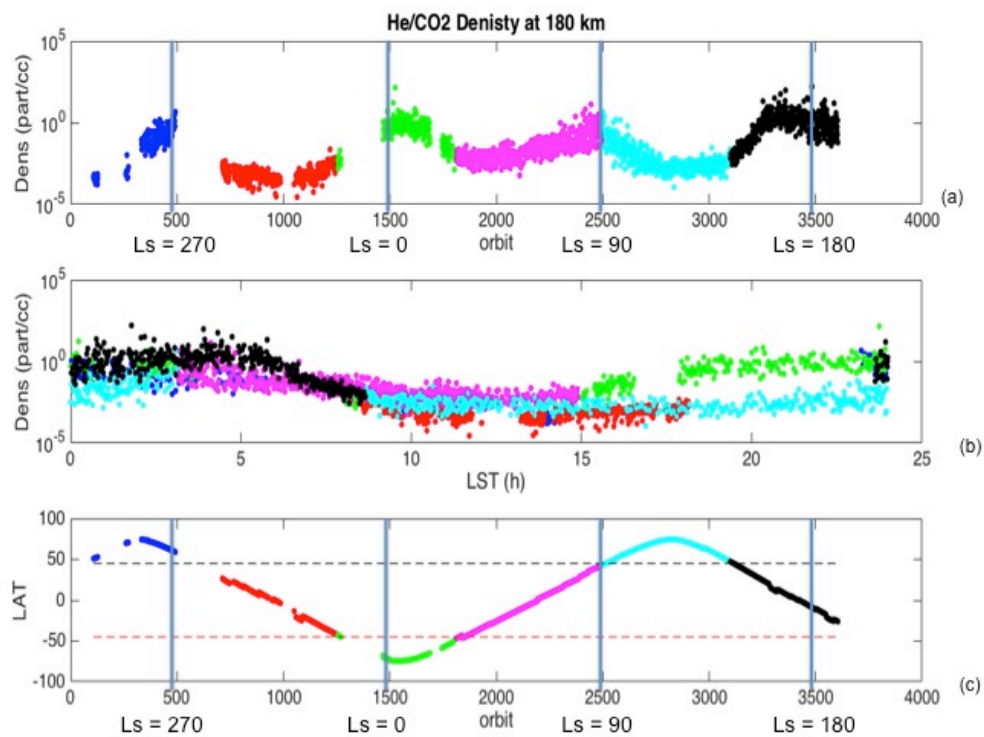


Figure 4—He/CO<sub>2</sub> Ratio over time: Vertical lines at  $L_s = 0, 90, 180,$  and  $270$ . Colors are consistent in each panel to allow tracking. (a) He/CO<sub>2</sub> ratio vs orbit. As CO<sub>2</sub> increases, He decreases, and vice-versa. The ratio is highest for highest He. (b) He/CO<sub>2</sub> ratio vs LST. The ratio peaks for LST = 2 – 5 h consistent with highest He densities. CO<sub>2</sub> is falling off as He is increasing in agreement with model results. This

demonstrates a He peak near dawn  $\sim 2 - 5$  h with a secondary peak around 20 h. This indicates much higher He densities and He/CO<sub>2</sub> ratio at dawn indicating a diurnal with a possible seasonal effect. (c) LAT vs. orbit number to illustrate the track of the orbit and track Ls.

One possible explanation for a larger southern polar He bulge at equinox vs the smaller northern polar He bulge at winter both occurring at night, could be an instrumental effect. Early in the mission NGIMS was originally set to operate with the filaments on high emission in order maximize neutral gas detection. In this mode, we discovered that the background on all mass channels ended up being much higher than anticipated, and backscattering effects from Ar and CO<sub>2</sub> near periapsis affecting lower mass channels was more significant than anticipated. Along with some other settings to mitigate the background, we elected to set the filaments on their lower setting in starting February 15 2015, just before the first deep dip pass. While this instrumentation effect was significant to the major species (CO<sub>2</sub>, Ar, N<sub>2</sub>, O, O<sub>2</sub>, CO), and the NGIMS team strongly recommends using data from February 14, 2015 onward, these initial settings had little impact on the detection of He. The impact on the CO<sub>2</sub> and Ar detection was significant and as a major component of the atmosphere and a major element in figure 3, it will affect the early data from the northern polar region only. No neutral data is available for any species including the lighter He from December 29, 2014 – February 14, 2015 due to this contamination issue. For this study we only used data with good pointing, and adequate signal above the noise for all species. In figure 3 & 4 it affects



blue dots up to the third large gap in data. Thus the first winter densities in the northern hemisphere may have a slightly higher background than all other densities, and the corrections for background may have abnormally lowered the densities for this small segment of data. Though He generally has a background near 0, CO<sub>2</sub> has a very high background and this was a much larger effect on the major species.

## **2.2—Methods: M-GITM**

The Mars Global Ionosphere-Thermosphere Model (M-GITM) is a model framework combining the terrestrial GITM framework [Ridley *et al.*, 2006] with Mars fundamental physical parameters, ion-neutral chemistry, and key radiative processes in order to capture the basic observed features of the thermal, compositional, and dynamical structure of the Mars atmosphere from the ground to ~250 km [Bougher *et al.*, 2015]. M-GITM simulates the conditions of the Martian atmosphere all the way to the surface, with an emphasis on upper atmosphere processes. Simulated three-dimensional upper atmosphere (80-250 km) fields include neutral temperatures, densities (CO<sub>2</sub>, CO, O, N<sub>2</sub>, O<sub>2</sub>, He, etc), winds (zonal, meridional, vertical), and photochemical ions (O<sup>+</sup>, O<sub>2</sub><sup>+</sup>, CO<sub>2</sub><sup>+</sup>, N<sub>2</sub><sup>+</sup> and NO<sup>+</sup>). Simulations spanning the full range of applications of the current M-GITM code, including 12 model runs spanning various solar cycle and seasonal conditions, have been completed and the results are described in a comprehensive initial paper [Bougher *et al.*, 2015].

The M-GITM upper atmosphere physics, chemistry, and formulations are the most complete, and therefore MAVEN data-model comparisons thus far have largely focused on this region above  $\sim 100$  km. At this point, M-GITM simulations have been compared with NGIMS measurements obtained during its first year of operations during four Deep Dip campaigns [Bougher *et al.*, 2015a; Bougher, 2015b]. In particular, Deep Dip 2 (DD2) temperatures and key neutral densities have been compared with corresponding M-GITM fields extracted along DD2 orbit trajectories on the dayside near the equator [Bougher *et al.*, 2015a]; a good match of key neutral densities and temperatures is revealed for nightside measurements.

The M-GITM model suggests that the He bulge will be strongest around the poles and weaker in the equatorial region. Slices of the global model at 200 km are taken at various seasons ( $L_s = 0, 90, 180$  and  $270$ ) as shown in Figure 5. These panels reveal a stronger bulge in the northern polar region ( $L_s = 270$ ), at mid-latitudes ( $L_s = 0$  &  $180$ ) and around the southern polar region ( $L_s = 90$ ) at LST = 2 – 5 h. These are global results, and when coverage from the MAVEN mission becomes more global, detailed He comparisons between NGIMS data and the model will be possible. Figure 6 compares LAT vs. LST (a) of He density for the entire year; conversely  $\text{CO}_2$  density for the entire year LAT vs. LST (b) all four panels at 200km. For certain configurations this compares well with the model, for others, more data is needed.

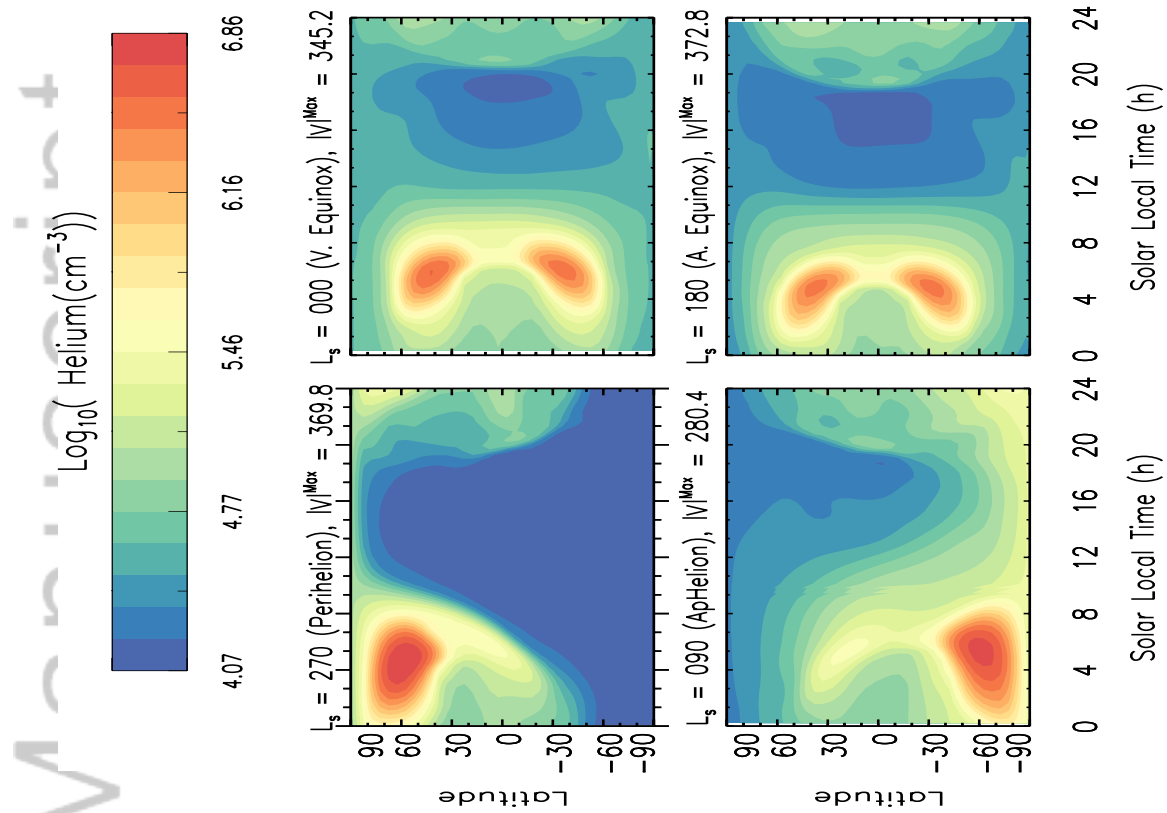


Figure 5—M-GITM results at a constant altitude of 200km shows LAT vs LST. Each panel represents a different slice at a different  $L_s$ ;  $L_s = 270$ ,  $L_s = 0$ ,  $L_s = 90$ , and  $L_s = 180$ . In each panel the He bulge occurs near  $L_s = 2 - 5$ , and shifts between the northern and southern poles with the seasons. As these are global model results it has complete coverage beyond MAVEN data coverage. Dark blue here is low counts as opposed to missing data.

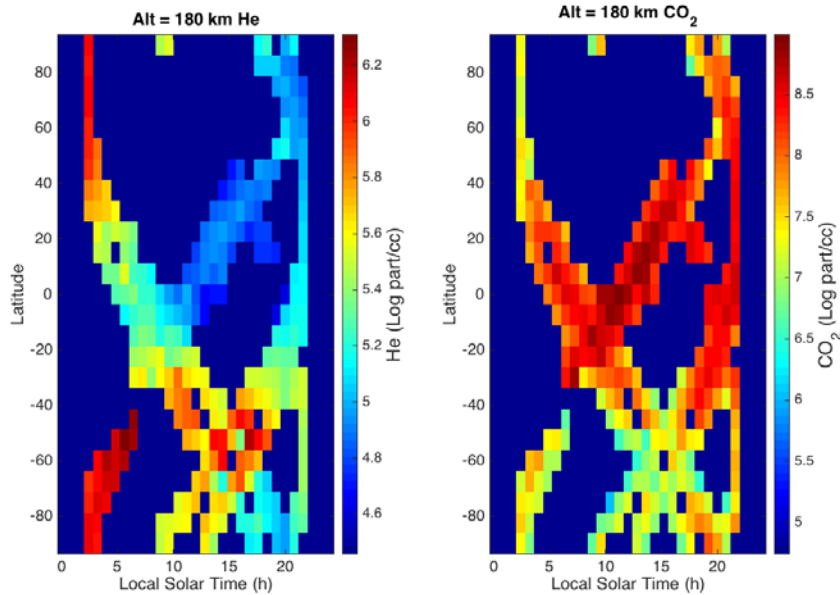


Figure 6—Constant altitude latitude vs LST: LAT vs. LST He density, and CO<sub>2</sub> density. He is highest at high latitudes, LST = 2 – 5 h. Since this is for the entire year and complete data set there are some similarities between the data set and the M-GITM model results. (Note: Dark blue indicates no data taken yet by MAVEN not just low counts, teal or light blue indicates lowest measured data)

While comparison between Figure 5 and 6 is difficult because coverage from MAVEN is still very incomplete it is possible to make some comparisons. Figure 6 shows a strong He bulge at LST = 2 – 5 h at the northern and southern polar regions. Additionally, between LST = 15 – 20 h is a secondary peak in the southern hemisphere. This secondary peak corresponds with Ls = 90 and Ls = 180 from figure 3 indicating that these occurred during equinox. While direct match between data and model is difficult due to coverage gaps, it is possible to observe nightside He accumulations and

enhancement of the He bulge at the poles vs. over the equatorial region as predicted by the model.

### 3—Discussion

With the MAVEN NGIMS measurements He bulges have now been discovered in the thermospheres of Earth, Venus and Mars [e.g. *Levine, Keating and Prior, 1974; Reber and Hays, 1973; Niemann et al., 1980*]. The seasonal responses of these bulges are most evident at Earth and Mars. At Earth, the He bulge has been found to be strongly seasonally dependent [*Liu et al., 2015; Sutton et al., 2015*]. It is highest at the poles in winter and lowest at summer. Terrestrial bulges have an enhancement feature associated with  $LST = 4$  at 400 km. Simulations from the three dimensional Thermosphere Ionosphere Electrodynamic GCM (TIEGCM) have shown that the large difference between the summer and winter He bulge is mostly dependent on local vertical advection and molecular diffusion [*Liu et al., 2014, Sutton et al., 2015*]. Early modeling efforts to describe the He bulge varied the eddy diffusion coefficients [*Kasnopolsky et al., 1994, Kasprzack et al., 1993*]. However, more recent modeling efforts found that vertical advection (connected to the interhemispheric circulation) has a stronger effect [*Liu et al., 2014*]. Specifically, seasonally varying horizontal winds indirectly contribute to the winter He bulge formation, as their divergence drives local vertical winds in order to satisfy mass continuity in the thermospheric general

circulation. As a light inert gas, Earth thermospheric He distributions are very sensitive to local vertical advection, especially in regions of convergence and downwelling of the thermospheric circulation (e.g winter polar regions). This makes He a sensitive tracer of the seasonally varying circulation pattern (and associated local vertical advection) for Earth.

The diurnal and seasonal effects on the He bulge for Mars indicate that there is possibly upward advection in the dayside summer hemisphere and downward advection in addition to the thermospheric circulation in the winter nightside creating the polar He bulges. As shown above for Mars, He densities are strongly enhanced for the nightside versus the dayside, revealing bulges at polar latitudes in and mid-latitudes (equinox) during early morning (LST = 2 – 5). Additionally, the two data sets from the northern polar region, (winter and summer) show approximately a factor of two difference in abundance between the nightside bulges indicating a seasonal enhancement in the northern polar region during the winter. As can be seen in figure 5, the model demonstrates that the diurnal effects in the polar regions at their peak, “winter”(Ls 270 or Ls 90) have an order of magnitude difference between night and dayside in agreement with the NGIMS data. At the lowest points, “summer”, the diurnal effects in the polar regions are much smaller, half and order magnitude to and order of magnitude. At the equinox, the diurnal bulges are reduced by half in both polar regions.

It is this combination that indicates not only that there should be a diurnal but also a seasonal effect according to the model. NGIMS data, thus far has found a smaller seasonal effect than the model predicts, which is likely largely due to lower coverage than needed to obtain the complete global picture from the M-GITM model.

Once again, it is likely that the global thermospheric circulation is primarily responsible with a secondary affect coming from vertical advective winds, consistent with dayside divergence (upwelling) and nightside convergence (downwelling) of the global wind pattern. Local nightside vertical advection produces a He bulge at the convergence (maximum downwelling) point of the circulation.

Since Mars indeed has seasons, the changing seasonal thermospheric circulation pattern is simulated by M-GITM [e.g. *Bougher et al.*, 2015], providing divergence on the dayside at mid-afternoon sub-solar latitudes, and convergence on the nightside. This nightside convergence point moves with season, resulting in polar enhancements of He in the winter hemisphere during the solstices, and mid-latitude enhancements of He densities during equinoxes. With Mars' larger eccentricity, the southern winter will be more pronounced than northern winter. This elongation of the southern winter season could also drag the He bulge south longer than the northern bulge delaying the transport north after southern winter. It is this delay that could help explain the much larger He bulge in the southern hemisphere at  $L_s = 0$  on the nightside over the He bulge

in the northern hemisphere near  $L_s = 270$  at the nightside. More modeling and measurement of Mars winds will continue to help explain these phenomena.

MAVEN NGIMS is in the process of measuring the upper atmosphere winds [Bougher *et al.*, 2016]. While direct measurements of the atmospheric winds are still pending, our results indicate that seasonally varying global winds yield seasonally varying downwelling winds (and vertical advection) that control the location and magnitude of the He bulge.

Conversely, Venus has no seasons, so this pattern is basically composed of a sub-solar to anti-solar circulation (stable), with a highly variable superimposed retrograde zonal (RSZ) component flow [e.g. Bougher *et al.*, 1997]. Resulting Venusian He densities are higher on the nightside (LST 2 – 5) than during the day near the equator, exactly opposite to the behavior for CO<sub>2</sub> densities [von Zahn *et al.*, 1983, Neimann *et al.*, 1980]. The mechanism for He bulge formation may be similar to Earth and Mars, with enhanced vertical advection at the convergence point (maximum downwelling winds) at the location of the bulge maximum. It is remarkable that the LST = 2 – 5 region for convergence in all Mars seasons is similar to that Venus. This similarity between Mars and Venus He bulge will help to explain the strong southern polar bulge occurring during equinox, which is unrelated to the seasonal effects noted at the northern polar region.

#### **4—Summary**



MAVEN NGIMS neutral measurements of He and CO<sub>2</sub> in the upper atmosphere of Mars revealed a peak in the He densities for LST = 2 – 5 h with a secondary peak around LST = 22 – 24 h. While He densities maximize on the nightside with an enhancement due to latitudinal (i.e. polar) and seasonal effects, NGIMS data also demonstrated that CO<sub>2</sub> densities were decreasing (dayside to nightside), similar to trends found at Venus. He bulges have been detected on Venus, Earth and now confirmed on Mars. The presence of a seasonal and diurnally dependent He bulge in the upper atmosphere is an indicator of strong local vertical advection (downwelling) in the nightside (often winter polar) thermosphere associated with the variable interhemispheric circulation pattern. He, being the lighter species, is driven primarily by the thermospheric circulation (and not the temperature distribution), inversely to that of the heavier elements like CO<sub>2</sub> and Ar. This is why there are larger He abundances on the nightside, especially at the polar regions than at the equatorial and dayside locations where CO<sub>2</sub> abundances are higher and He is lower.

## **5—Acknowledgments**

Special acknowledgments to the MAVEN NGIMS team at NASA Goddard SFC, and the MAVEN operations team at LASP and Lockheed Martin in Colorado. All data are archived

in the Planetary Atmospheres Node of the Planetary Data System (<http://pds.nasa.gov>).

Data through August 15, 2016 is available on the Planetary Data System (PDS4) (e.g.

*mvn\_ngi\_l2\_csn-abund-14015\_20141018T100458\_v06\_r02.csv*

*mvn\_ngi\_l2\_cso-abund-20708\_20160804T173834\_v06\_r02.csv*).

These data are available upon request. The MAVEN mission has been funded by NASA through the Mars Exploration Program.

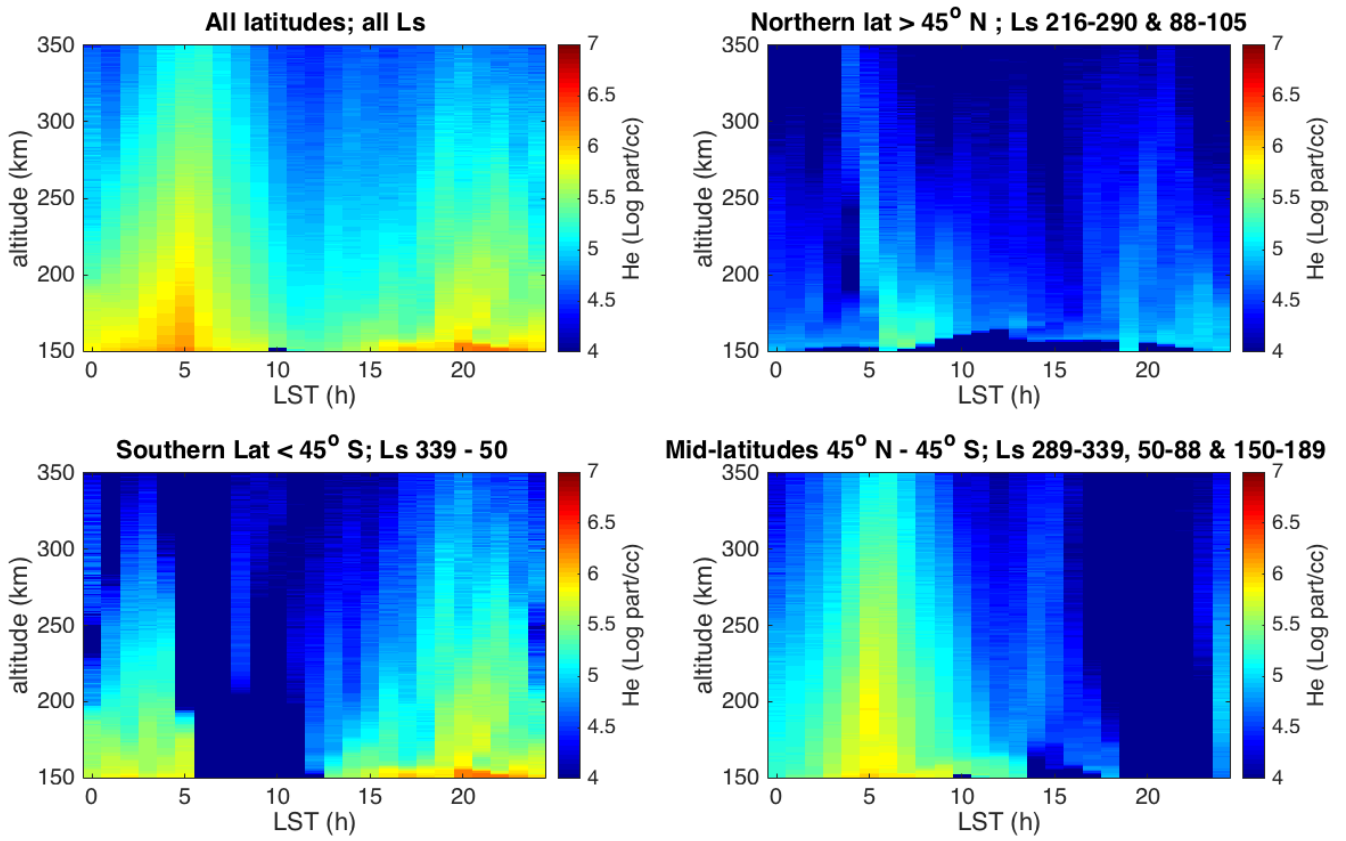
## References

- Bell, J.M., Bougher, S.W., Mahaffy, P.M., Elrod, M.K.(2015), Simulating Helium Abundances in the Martian Upper atmosphere using 1-D and 3-D models. *AAS DPS meeting #47 id 419.21*.
- Bougher, S. W., M. J. Alexander, and H. G. Mayr, (1997), Chapter 9: Upper atmospheric dynamics: Global circulation and gravity waves, *in Venus II: Geology, Geophysics, Atmosphere, and Solar Wind Environment*, Eds. S. W. Bougher, D. M. Hunten, and R. J. Phillips, U. of Arizona Press.
- Bougher, S.W., Dickenson, R.E., Ridley, E.C., Roble, R.G., (1988). Venus mesosphere and thermosphere: III. Three-dimensional general circulation with coupled dynamics and composition, *Icarus*, 73, 545-573, doi:10.1016/0019-1035(88)90064-4
- Bougher, S.W., Roble, R., (2003), Helium as a tracer of terrestrial planet upper atmosphere dynamics : Predictions for Mars, *AGU abstract*
- Bougher, S. W., B. M. Jakosky, J. Halekas, J. Grebowsky, J. G. Luhmann, and others, Early MAVEN dip deep campaign reveals thermosphere and ionosphere variability, *Science*, 350, 1–7, (2015a) doi:doi:10.1126/science.aad0459.
- Bougher, S. W., J. M. Bell, K. Olsen, K. Roeten, P. R. Mahaffy, M. Elrod, M. Benna, and B. M. Jakosky, (2015b) Variability of Mars thermospheric neutral structure from MAVEN deep dip observations: NGIMS comparisons with global models, *EOS*, 2015 Supplement(74805)
- Bougher, S. W., R. G. Roble, E. C. Ridley, and R. E. Dickinson (1990), The Mars Thermosphere .2. General-Circulation with Coupled Dynamics and Composition, *J Geophys Res-Solid*, 95(B9), 14811-14827, doi:Doi 10.1029/Jb095ib09p14811.

- Bougher, S.W., Roeten, K.J., Olsen, K.G., Mahaffy, P.R., Benna, M., Elrod, M.K., Bell, J.M., Jakosky, B.M., (2016) Variability of the Thermospheric Wind Structure of Mars: MAVEN NGIMS Measurements and Corresponding Global Model Simulations, *AGU Fall Meeting* P13D-05
- Cageao, R.P. and R.B. Kerr, (1984), Global distribution of helium in the upper atmosphere during solar minimum, *Planetary Space Science*, vol. 32, iss. 12, pp1523-1529. doi:10.1016/0032-0633(84)90019-9
- Hartle, R. E., T. M. Donahue, J. M. Grebowsky, and H. G. Mayr (1996), Hydrogen and deuterium in the thermosphere of Venus: Solar cycle variations and escape, *J. Geophys. Res.*, 101(E2), 4525–4538, doi:10.1029/95JE02978.
- Jakosky, B. M., R. P. Lin, J. M. Grebowsky, J. G. Luhmann, D. F. Mitchell, G. Beutelschies, and others (2014), The Mars Atmosphere and Volatile Evolution (MAVEN) Mission, *Space Sciences Reviews*, doi:10.1007/s11214-015-0139-x.
- Kasprzak, W.T., Neiman, H.B., Hedin, A.E., (1993), Neutral Composition Measurements by the Pioneer Venus Neutral Mass Spectrometer During Orbiter Re-Entry, *GRL*, vol 20, 2747-2750, DOI: 10.1029/93GL02241
- Kasprzak, W. T. (1969), Evidence for a helium flux in the lower thermosphere, *J. Geophys. Res.*, 74(3), 894–896, doi:10.1029/JA074i003p00894.
- Keating, G.M., Bougher, S., (1987) Neutral Upper Atmospheres of Venus and Mars, *Adv. Space Res.* Vol 7, No. 12 pp. 12(57) – (12)71, doi:10.1016/0273-1177(87)90202-X.
- Kockarts, G. *Space Sci Rev* (1973) 14: 723. doi:10.1007/BF00224775.
- Krasnopolsky, V.A., Bowyer, S., Chakrabarti, S., Gladstone, G.R., McDonald, J.S., (1994), First Measurement of Helium on Mars: Implications for the Problem of Radiogenic Gases on the Terrestrial Planets, *Icarus*, 109 p 337-351, doi:10.1006/icar.1994.1098
- Krasnopolsky, V. A., Mars' upper atmosphere and ionosphere at low, medium, and high solar activities: Implications for evolution of water, *J. Geophys. Res.*, 107(E12), 5128, doi:10.1029/2001JE001809, 2002.
- Krasnopolsky, V. A., and G. R. Gladstone (1996), Helium on Mars: EUVE and PHOBOS data and implications for Mars' evolution, *J. Geophys. Res.*, 101(A7), 15765–15772, doi:10.1029/96JA01080.,
- Krasnopolsky, V. A., S. Chakrabarti, and G. R. Gladstone (1993), Helium in the Martian atmosphere, *J. Geophys. Res.*, 98(E8), 15061–15068, doi:10.1029/93JE00534.
- Krasnopolsky, V.A., Gladstone, G.R., (2005), Helium on Mars and Venus: EUVE observations and modeling, *Icarus*, 176 p 395-407 DOI: 10.1029/93GL02241
- Liu, X., W. Wang, J. P. Thayer, A. Burns, E. Sutton, S. C. Solomon, L. Qian, and G. Lucas (2014), The winter helium bulge revisited, *Geophys. Res. Lett.*, 41, 6603–6609, doi:10.1002/2014GL061471.

- Levine, J. S., G.M., Keating, E.J Prior, (1974) Helium in the Martian atmosphere: Thermal loss considerations, *Planerat Space Science*, vol 22, iss3, pp 500-503, doi:10.1016/0032-0633(74)90082-8
- Mahaffy, P. R., M. Benna, M. Elrod, R. V. Yelle, S. W. Bougher, S. W. Stone, and B. M. Jakosky (2015), Structure and composition of the neutral upper atmosphere of Mars from the MAVEN NGIMS investigation, *Geophysical Research Letters*, 42(21), 8951-8957, doi:10.1002/2015GL065329.
- Mahaffy, P. R., et al. (2014), The Neutral Gas and Ion Mass Spectrometer on the Mars Atmosphere and Volatile Evolution Mission, *Space Science Reviews*, 195(1), 49-73, doi:10.1007/s11214-014-0091-1.
- Niemann, H. B., W. T. Kasprzak, A. E. Hedin, D. M. Hunten, and N. W. Spencer (1980), Mass spectrometric measurements of the neutral gas composition of the thermosphere and exosphere of Venus, *J. Geophys. Res.*, 85(A13), 7817–7827, doi:10.1029/JA085iA13p07817.
- Neir, A.O and McElrod, M.B., (1977) Composition and structure of Mars' upper atmosphere – Results from the neutral mass spectrometers on Viking 1 and 2, *J. Geophys. Res.*, 82, 4341-4349, doi:10.1029/JS082i028p04341.
- Reber, C. A., and P. B. Hays (1973), Thermospheric wind effects on the distribution of helium and argon in the Earth's upper atmosphere, *J. Geophys. Res.*, 78(16), 2977–2991, doi:10.1029/JA078i016p02977.
- Ridley, A., Y. Deng, and G. Toth, (2006) The global ionosphere-thermosphere model, *J. Atmos. Sol-Terr. Phys.*, 68, 839, <http://dx.doi.org/10.1016/j.jastp.2006.01.008>.
- Roble, R.G., E.C. Ridley, A.D. Richmond, R.E. Dickinson, (1988), A coupled thermosphere/ionosphere general circulation model, *GRL*, vol 15, Issue12, p 1325-1328. DOI: 10.1029/GL015i012p01325.
- Sutton, E. K., J. P. Thayer, W. Wang, S. C. Solomon, X. Liu, and B. T. Foster (2015), A self-consistent model of helium in the thermosphere, *J. Geophys. Res. Space Physics*, 120, 6884–6900, doi:10.1002/2015JA021223.
- Von Zahn, U., S. Kumar, H. Niemann, and R. Prinn, Chapter 13: Composition of the Venus Atmosphere, in *Venus Book*, Eds. D. M. Hunten, L. Colin, T. M. Donahue, and V. I.

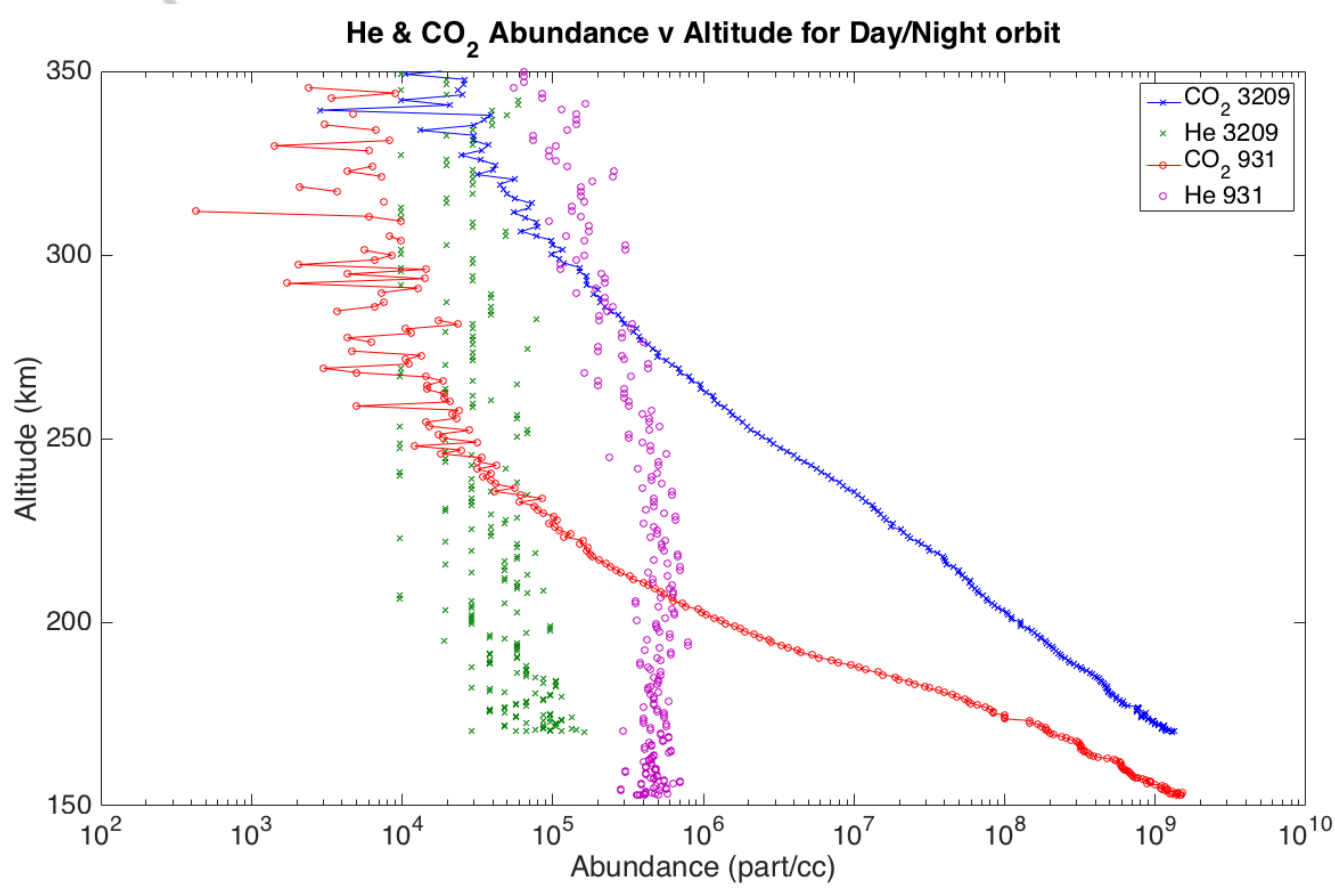
ript



2016JA023482-f01-z.tif

Au

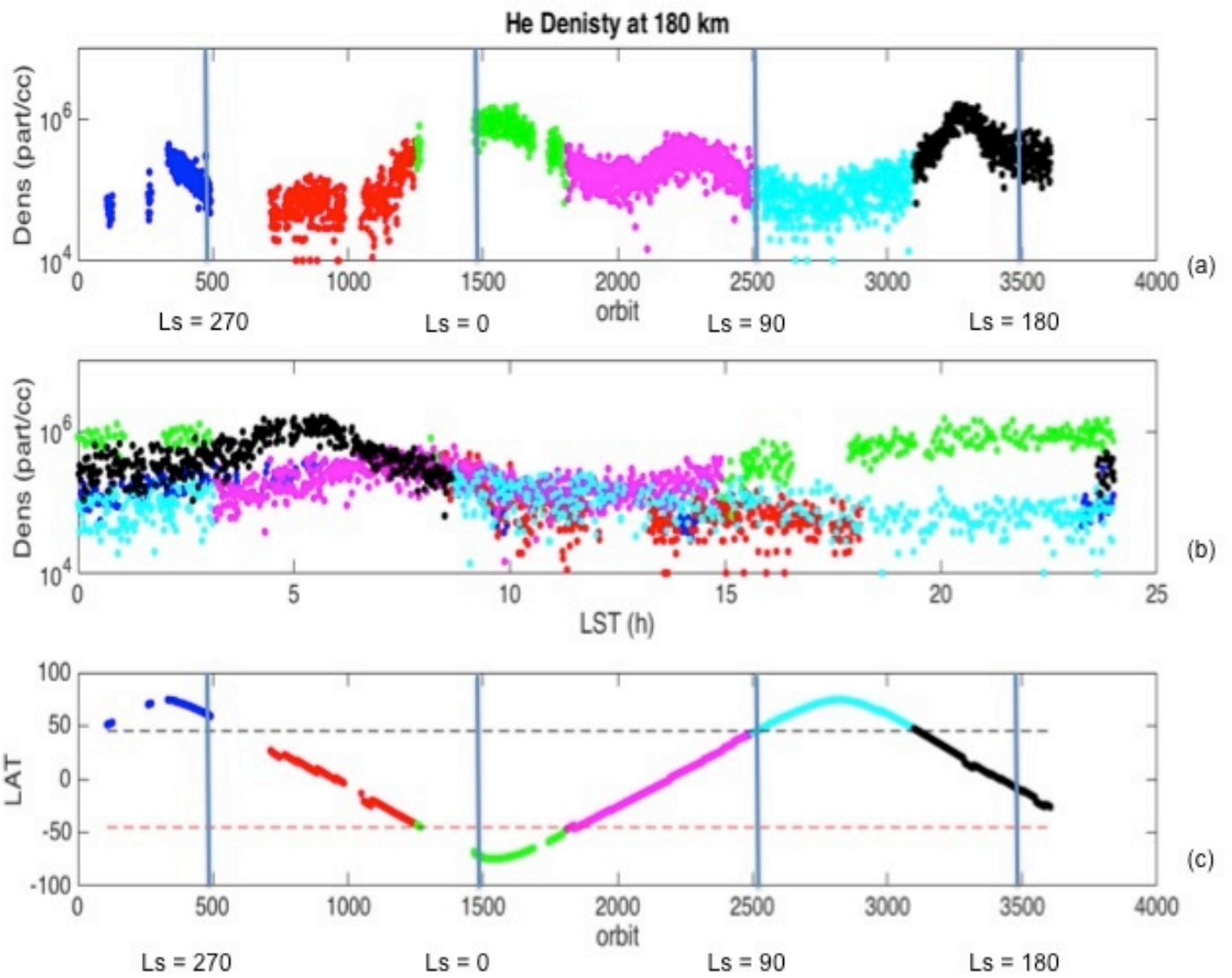
ript



2016JA023482-f02-z-.tif

Au

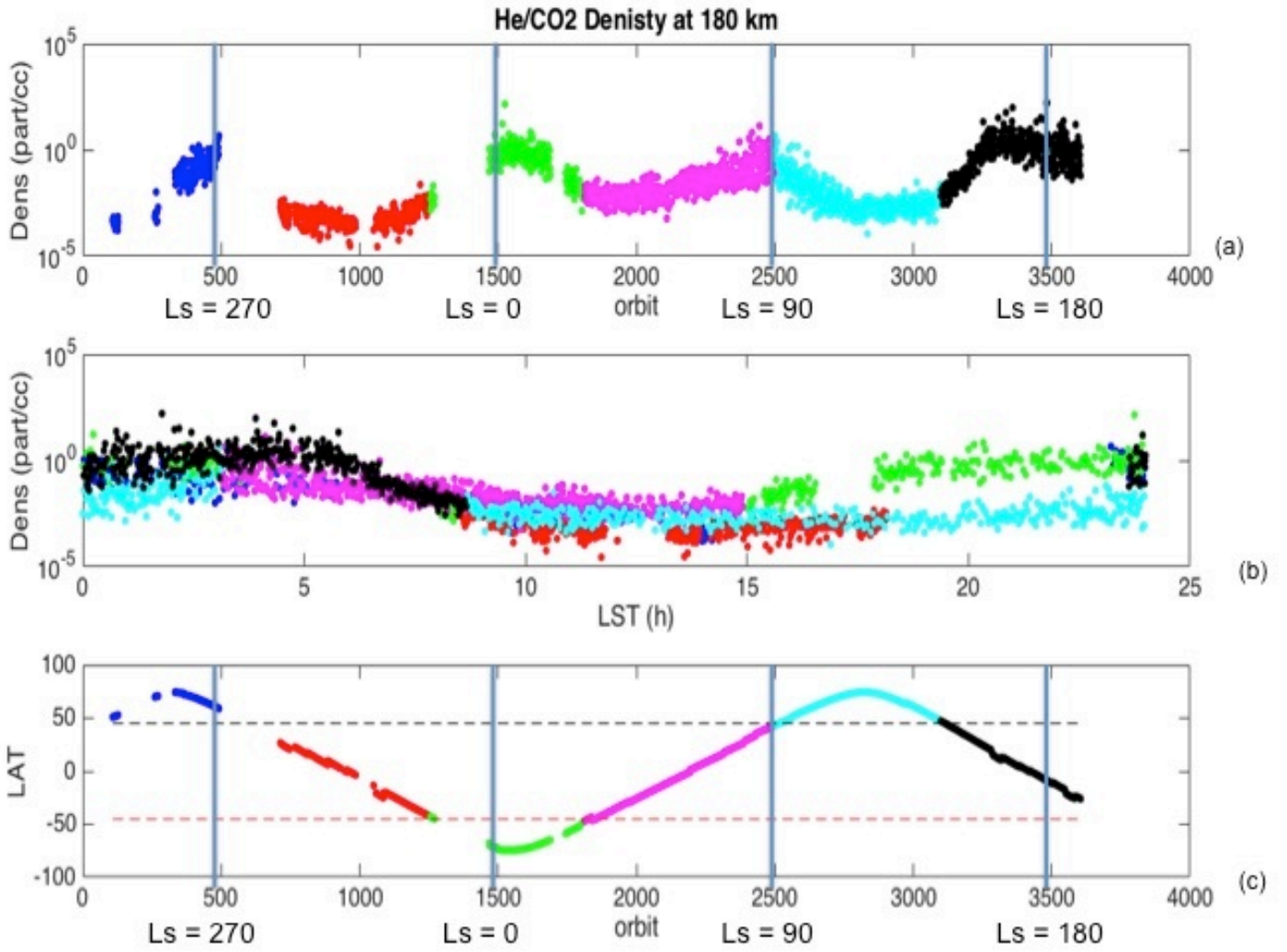
t



A

2016JA023482-f03-z-jpg

ct



A

2016JA023482-f04-z-jpg



$\text{Log}_{10}(\text{ Helium}(\text{cm}^{-3}))$



4.07

4.77

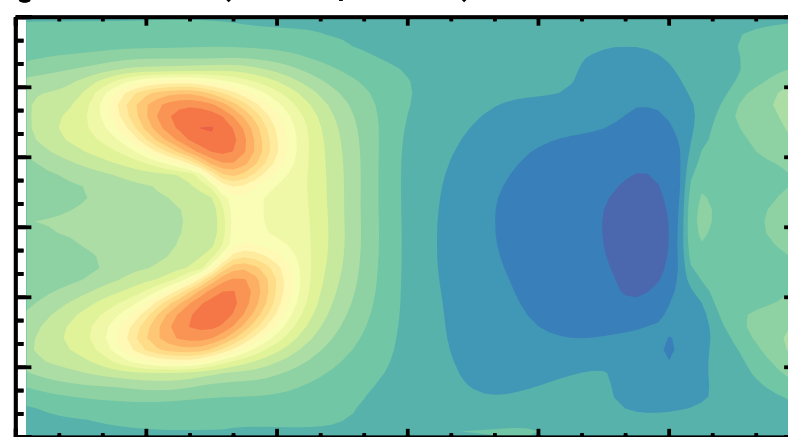
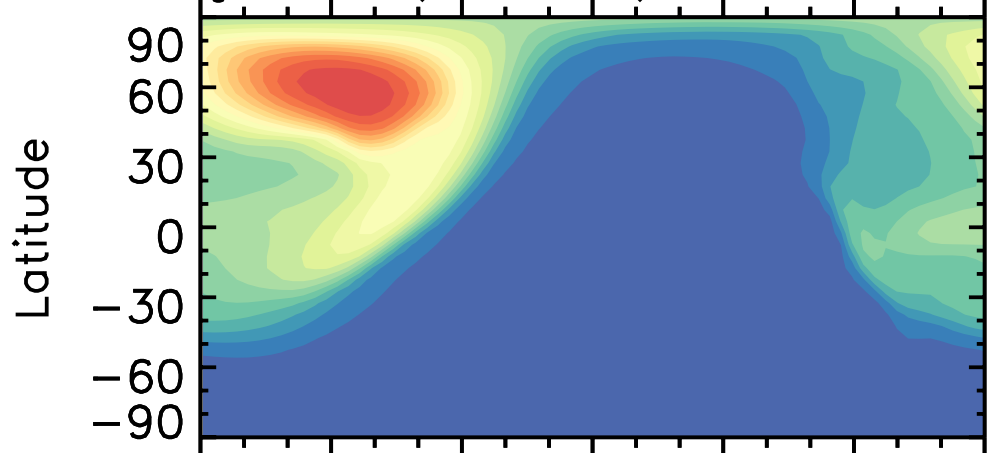
5.46

6.16

6.86

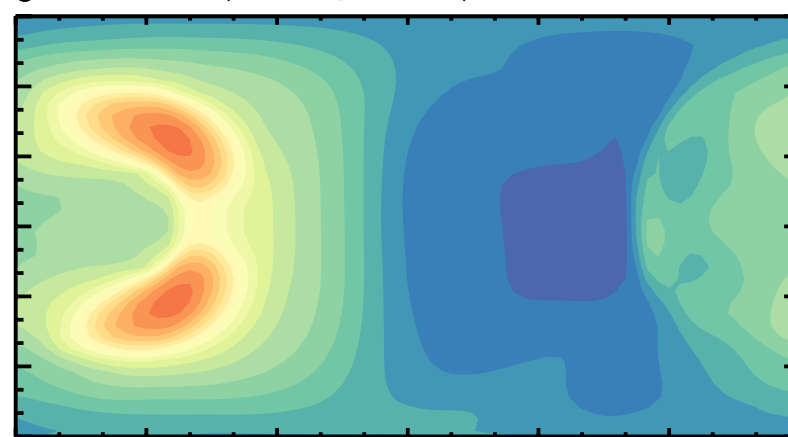
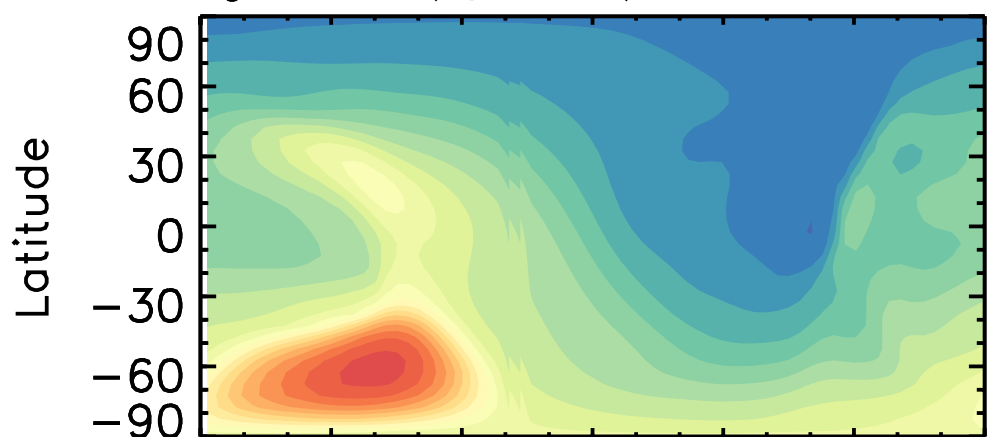
$L_s = 270$  (Perihelion),  $|V|^{Max} = 369.8$

$L_s = 000$  (V. Equinox),  $|V|^{Max} = 345.2$



$L_s = 090$  (ApHelion),  $|V|^{Max} = 280.4$

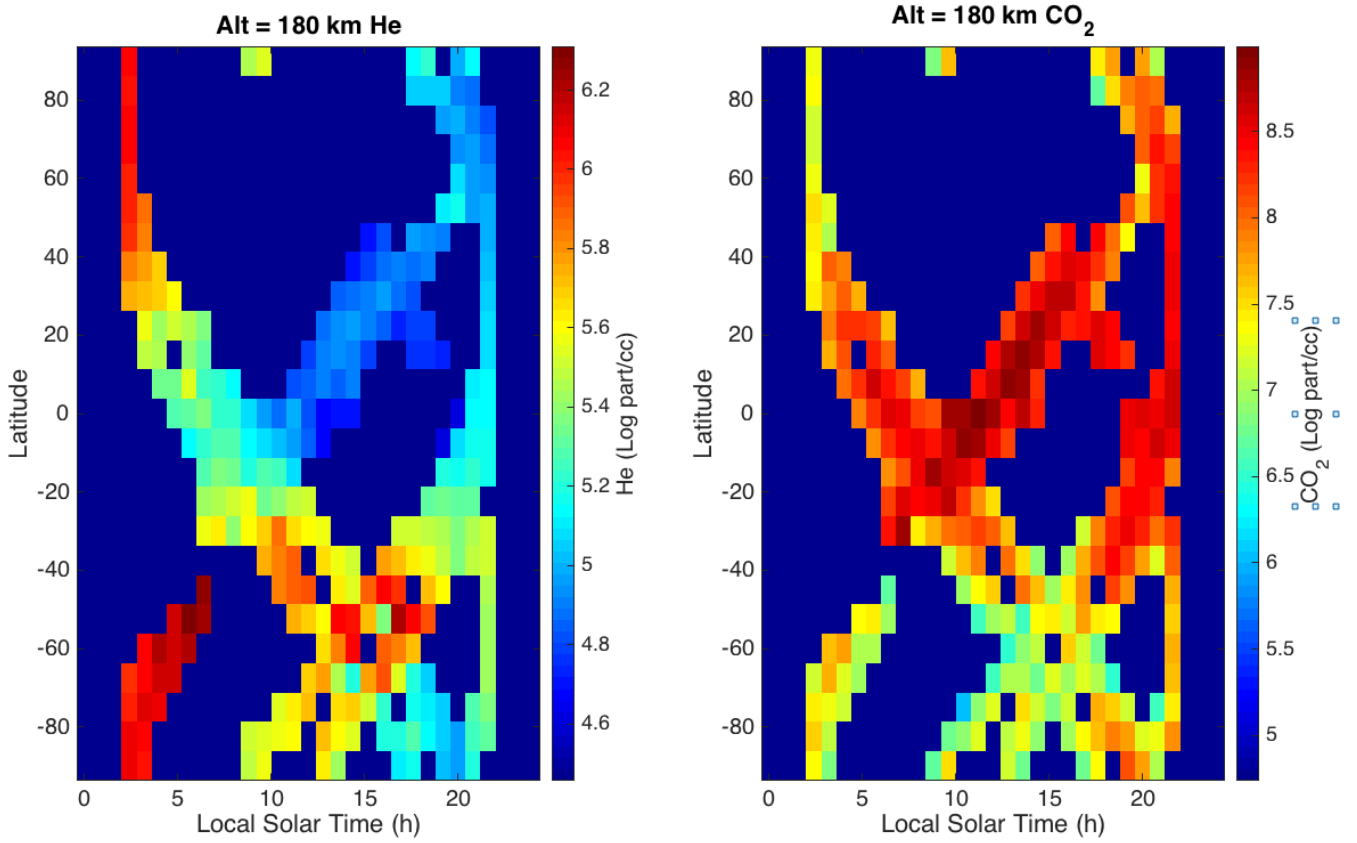
$L_s = 180$  (A. Equinox),  $|V|^{Max} = 372.8$



0 4 8 12 16 20 24

0 4 8 12 16 20 24

ript



2016JA023482-f06-z-.tif

Aut